http://dx.doi.org/10.5755/j01.eie.23.3.18326 ELEKTRONIKA IR ELEKTROTECHNIKA, ISSN 1392-1215, VOL. 23, NO. 3, 2017

# Maxwell-Equations Based on Mining Transient Electromagnetic Method for Coal Mine-Disaster Water Detection

Benyu Su[1], Jingcun Yu[1], Chenxing Sheng[2], Yulei Zhang[3]
[1]*School of Resource and Geoscience, China University of Mining and Technology, No. 1, Daxue Road, Xuzhou, Jiangsu, 221116, P. R. China*
[2]*School of Power & Energy Engineering, Wuhan University of Technology, Wuhan, 430063, China*
[3]*China National Oil and Gas Exploration and Development Corporation Beijing, 100034,China*
*yjccumt@gmail.com*

***Abstract*—Water-bearing geological structure is a serious threat to coalmine safety. This research focuses on detecting water-bearing geological structure by transient electromagnetic method. First, we introduce the principle of mining transient electromagnetic method, and then explain the technique of Finite Different Time Domain using in the transient electromagnetic method. Based on Maxwell equations, we derive the difference equations of electromagnetic field and study the responses of water-bearing geological structure using FDTD. Moreover, we establish the relationship between receiving electromagnetic field and geological information. The typical coal geological model of goaf-water is chosen to do the numerical simulation. Besides, we verify the availability of the method by numerical simulation using coal geological model. Finally, we use the method in the coalmine which is located in Linfen city in Shanxi province in China, and the detecting result is verified by drilling.**

***Index Terms*—Maxwell equations; FDTD; coalmine; transient electromagnetics.**

## I. INTRODUCTION

Transient Electromagnetic Method (TEM) used in coalmine is called Mining Transient Electromagnetic Method (MTEM). The MTEM is used to locate the source of mine water, which is one of the main disasters in coalmine production and construction. There are three locations of mine water, i.e., roadway roof, roadway floor, and roadway lateral wall/head (Fig. 1). According to the records [1], more than 80 % of water disasters occur at the heading face of coal roadway. Although the counts of water disaster in heading face is much more than that in roof, floor and lateral wall, the detection of the disaster water source are still an important issue.

Due to that the roadway environment mainly refers its narrow space and metal interference, traditional geophysical methods are inefficient for water disaster detection in roadway. At present, the geophysical exploration methods are popular to predict coalmine water disaster. Representative geophysical method include mine direct current method [2], radio wave penetration method, audio frequency electric penetration method and mine transient electromagnetic method (MTEM) [3]. Among these methods, MTEM is widely used in the detection of advanced heading face. The reason is that it has the following advantages: easy taken in the roadway, sensitivity to water-bearing structures, easy operation and small time consuming. Though many researchers have been studied TEM, they mainly focused on the ground surface [4], marine [5] and air [6]. In addition, few researches can be found in literature related with coalmine roadway. Here, we introduce the principle of MTEM to interpret its application in the coalmine.

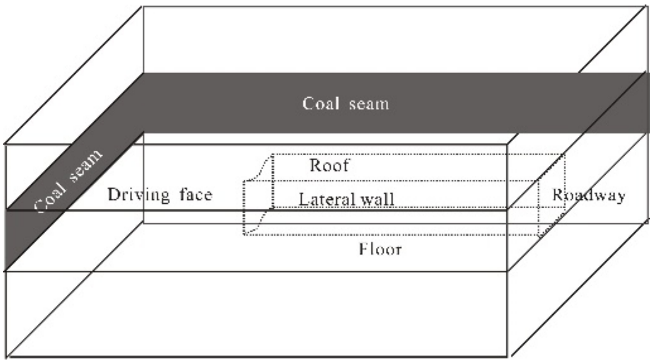


Fig. 1. Geological model of coalmine roadway.

As mentioned above, the difference between ground surface TEM and MTEM is that the measurement of MTEM is located in the mine roadway. The transmitter carrying current will result in primary magnetic field which is called the first field. When the current is abruptly turned off, the change of primary magnetic field will induce eddy current in the conductor. The eddy current will result in a magnetic field, called the second field. The receiver loop will record the second field, as shown in Fig. 2. The information of the earth can be obtained from the second field. In order to transmit the signal with enough power and in order to receive the expected information, the multi-turn minor loop devices were proposed by our previous work [7]. In the mine roadway, we can detect

Manuscript received 11 December, 2016; accepted 21 April, 2017.
This work was supported by A Project Funded by the Priority Academic Program Development of Jiangsu Higher Education Institutions and the Fundamental Research Funds for the Central Universities 2014QNA88.

the information of roof, floor and heading of coal seam by adjusting loops detection directions (Fig. 6). Besides, we can detect different directions in the same surface, as shown in Fig. 3.

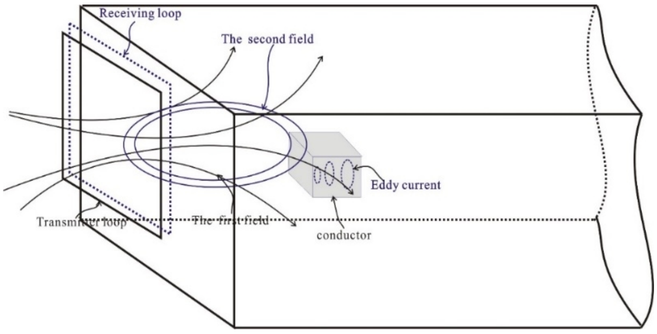


Fig. 2. Principle of TEM.

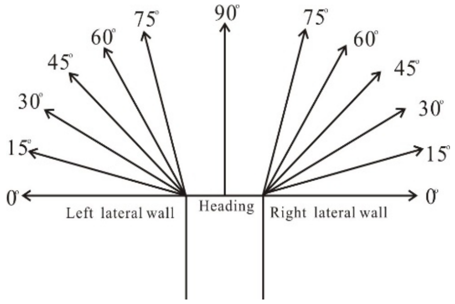


Fig. 3. Detecting directions in the same horizental section in the coalmine roadway.

## II. PRINCIPLE OF MTEM

Under the quasi-static condition and in source-free, isotropic, and non-magnetic medium, Maxwell differential equations [8] can be expressed as:

$$-\frac{\partial \vec{B}}{\partial t} = \nabla \times \vec{E}, \tag{1}$$

$$\sigma \vec{E} = \nabla \times \vec{H}, \tag{2}$$

$$\nabla \times \vec{B} = 0, \tag{3}$$

$$\nabla \times \vec{J} = 0, \tag{4}$$

where $B$ is the magnetic induction, $H$ is the magnetic field intensity, $E$ is the electric field intensity, $\sigma$ is the conductivity of the medium and $J$ is the conduction current density.

Equation (2) can be modified by plus the item of time, as shown in equation (5), which can simplify the requirements of solving equation [9]

$$\gamma \frac{\partial \vec{E}}{\partial t} + \sigma \vec{E} = \nabla \times \vec{H}, \tag{5}$$

where $\gamma$ is the ghost permittivity [10].

Equation (5) can be rewritten by the form of three components:

$$\gamma \frac{\partial \vec{E}_x}{\partial t} + \sigma \vec{E}_x = \frac{\partial \vec{H}_z}{\partial y} - \frac{\partial \vec{H}_y}{\partial z}, \tag{6}$$

$$\gamma \frac{\partial \vec{E}_y}{\partial t} + \sigma \vec{E}_y = \frac{\partial \vec{H}_x}{\partial z} - \frac{\partial \vec{H}_z}{\partial x}, \tag{7}$$

$$\gamma \frac{\partial \vec{E}_z}{\partial t} + \sigma \vec{E}_z = \frac{\partial \vec{H}_y}{\partial x} - \frac{\partial \vec{H}_x}{\partial y}. \tag{8}$$

Due to the form of electromagnetic field, many researchers [11] adopt 3-D FDTD to solve Maxwell equations, the earth model is discretized into Yee unit model, as shown in Fig. 4. In the model, the electric field components are located at the centers of the prism edges with their directions parallel to the prism edges, and the magnetic field components are located at the centers of the prism faces with their directions parallel to the normal directions of the faces.

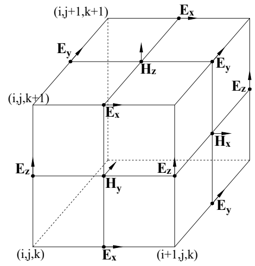


Fig. 4. Position of each field component in a discretized Yee unit.

The iterative equation for electric and magnetic fields, and specific discrete process and difference equation can be obtained by applying component forms of (1) and (5) and using central difference to perform approximate discretization [9].

In order to calculate the z-component of the magnetic field for the whole space, we should maintain the symmetry of fields in whole space. Hence, first, the following equation can be obtained from (1)

$$-\frac{\partial \vec{B}_z}{\partial t} = \frac{\partial \vec{E}_y}{\partial x} - \frac{\partial \vec{E}_x}{\partial y}. \tag{9}$$

Then, from (3), we can get

$$\frac{\partial \vec{B}_z}{\partial z} = -\frac{\partial \vec{B}_x}{\partial x} - \frac{\partial \vec{B}_y}{\partial y}. \tag{10}$$

In the whole space model, the source is located at the centre of the model, which is often taken as the origin of coordinates. In calculation, $\vec{B}_z$ value of each unit on the plane where the origin is located (namely, the plane z = 0) is first calculated by using (9). Then, z-components of the magnetic field at other positions are calculated by using (10). By using central difference, (9) can be discretized as follows

$$\vec{B}_z^{n+\frac{1}{2}}\left(\mathrm{i}+\frac{1}{2}, \mathrm{j}+\frac{1}{2}, \mathrm{k}\right) = \vec{B}_z^{n-\frac{1}{2}}\left(\mathrm{i}+\frac{1}{2}, \mathrm{j}+\frac{1}{2}, \mathrm{k}\right) - \frac{\Delta t_{n-1} + \Delta t_n}{2} \times$$
$$\times \left[ \frac{\vec{E}_y^n\left(\mathrm{i}+1, \mathrm{j}+\frac{1}{2}, \mathrm{k}\right) - \vec{E}_y^n\left(\mathrm{i}, \mathrm{j}+\frac{1}{2}, \mathrm{k}\right)}{\Delta x_i} - \right.$$
$$\left. - \frac{\vec{E}_x^n\left(\mathrm{i}+\frac{1}{2}, \mathrm{j}+1, \mathrm{k}\right) - \vec{E}_x^n\left(\mathrm{i}+\frac{1}{2}, \mathrm{j}, \mathrm{k}\right)}{\Delta y_j} \right]. \tag{11}$$

Equation (10) can be discretized as:

$$\vec{B}_z^{n+\frac{1}{2}}\left(i+\frac{1}{2}, j+\frac{1}{2}, k\right) = \vec{B}_z^{n+\frac{1}{2}}\left(i+\frac{1}{2}, j+\frac{1}{2}, k+1\right) + \Delta z_k \times \left[\frac{\vec{B}_x^{n+\frac{1}{2}}\left(i+1, j+\frac{1}{2}, k+\frac{1}{2}\right) - \vec{B}_x^{n+\frac{1}{2}}\left(i, j+\frac{1}{2}, k+\frac{1}{2}\right)}{\Delta x_i} + \frac{\vec{B}_y^{n+\frac{1}{2}}\left(i+\frac{1}{2}, j+1, k+\frac{1}{2}\right) - \vec{B}_y^{n+\frac{1}{2}}\left(i+\frac{1}{2}, j, k+\frac{1}{2}\right)}{\Delta y_j}\right], \tag{12}$$

$$\vec{B}_z^{n+\frac{1}{2}}\left(i+\frac{1}{2}, j+\frac{1}{2}, k\right) = \vec{B}_z^{n+\frac{1}{2}}\left(i+\frac{1}{2}, j+\frac{1}{2}, k-1\right) - \Delta z_k \times \left[\frac{\vec{B}_x^{n+\frac{1}{2}}\left(i+1, j+\frac{1}{2}, k-\frac{1}{2}\right) - \vec{B}_x^{n+\frac{1}{2}}\left(i, j+\frac{1}{2}, k-\frac{1}{2}\right)}{\Delta x_i} + \frac{\vec{B}_y^{n+\frac{1}{2}}\left(i+\frac{1}{2}, j+1, k-\frac{1}{2}\right) - \vec{B}_y^{n+\frac{1}{2}}\left(i+\frac{1}{2}, j, k-\frac{1}{2}\right)}{\Delta y_j}\right]. \tag{13}$$

In the iteration, $\vec{B}_z$ value of each unit on the plane where the source is located (namely, the plane z = 0) is first calculated by using (10). Then, $\vec{B}_z$ values of units located in the areas, z < 0 and z > 0, are calculated using (12) and (13). This discrete way ensures the fields are symmetric about the plane z = 0. In addition, it does not only add the constraint conditions of (3) to the iteration process, but also makes $\vec{B}_z$ values free from the influence of boundary conditions. Therefore, it is of high accuracy.

After calculation of *B*, we will express induction voltage $\varepsilon(t)$ by the formula [7]

$$\varepsilon(t) = n \times s \times \frac{\partial \vec{B}}{\partial t}. \tag{14}$$

where, *n* is the number of turns and *s* is the area of the receiver loop.

In order to describe the resistivity of the earth, we transform the induction electromotive force into resistivity information via (15) [7]

$$\rho_a = \frac{\mu_0}{4\pi t}\left(\frac{2\mu_0 SNsn}{5t(\varepsilon(t)/I)}\right)^{\frac{2}{3}}, \tag{15}$$

where $\rho_a$ is the apparent resistivity, *S* is the area of transmit loop and *N* is the turn number of transmit loop, *n* is the number of turns and *s* is the area of the receiver loop, $u_0$ is the magnetic permeability, *I* is the current value and *t* is measurement time.

## III. NUMERICAL SIMULATION

Goaf filled with water is the common source of water inrush in the roadway. By taking goaf filled with water as an example, we study the responses of transmits electromagnetic in the whole space. A three-dimensional whole-space coal geological model was established, as shown in Fig. 5. In the model, resistivity of coal seam was set as 400 Ω·m and the resistivity of surrounding rock is defined to be 200 Ω·m. Besides, thickness of coal seam was set to be 10 m. The volume of goaf is 30 m × 30 m × 30 m and the resistivity is defined as 1Ω·m. Besides, the measuring points around the roadway head were arranged at various angles from 0 degree to 180 degree. As shown in the Fig. 6(a), Fig. 6(b) and Fig. 6(c) indicate that detecting information of floor, front and roof by adjusting the detection direction and the corresponding results are shown in Fig. 6(A), Fig. 6(B) and Fig. 6(C) which are apparent resistivity contours. Here, there is obvious abnormal character in Fig. 6(B) and the abnormal area indicates low resistivity which coincide with geological model.

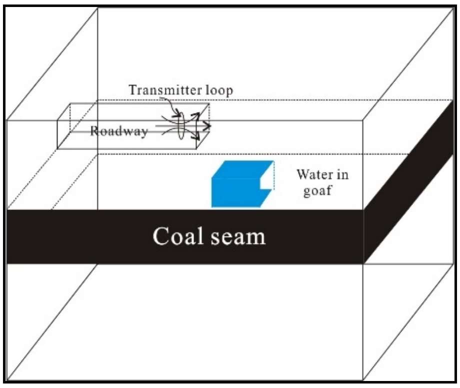


Fig. 5. The geological model of coal.

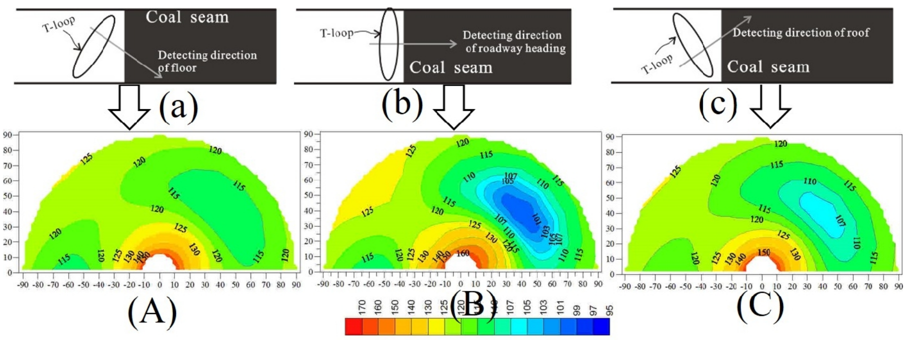


Fig. 6. The numerical modelling result.

## IV. EXPERIMENTAL RESULTS

The coalmine was located in Henlong town in Linfen City in Shanxi Province, as shown in Fig. 7.

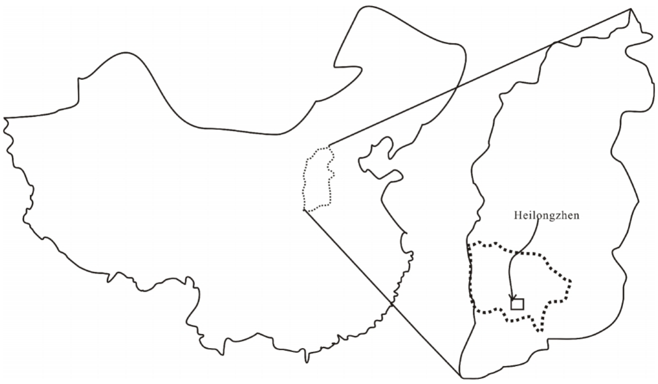


Fig. 7. The location of coalmine.

The character of coal geology is dominated by karst fissures, which corresponds to a very serious problem. Besides, there are many collapse columns, which usually develop into the path of conducted water. Hence, the advanced prospecting is very necessary before coal mining. Hence, we carry out the detection in the coalmine roadway, as shown in Fig. 8 which is the photo of measurement in the coalmine roadway. Furthermore, Fig. 9 shows the prospecting results. From the prospecting results, we can analyse that the location with a low resistivity abnormal geological body represents a water bearing collapse column, which is verified by geological drilling.

Fig. 8. Measurement of MTEM in the coalmine roadway.

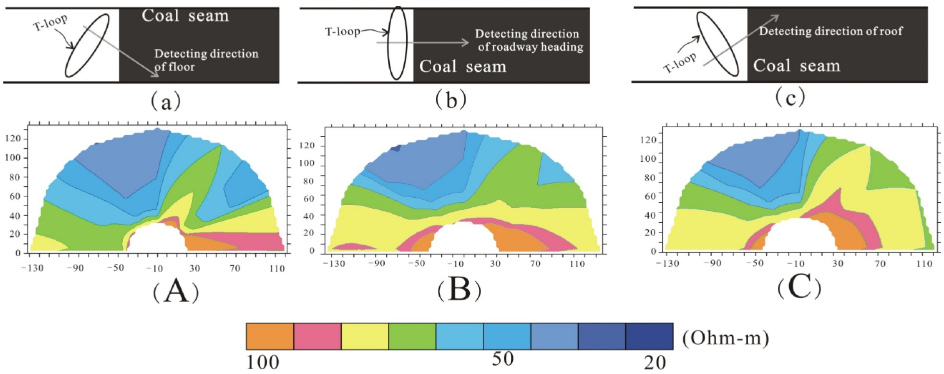


Fig. 9. The measurement results.

## V. CONCLUSIONS

In this paper, we present a new application of geophysical method into disaster water source detection in coalmine roadway, based on electromagnetic principles. Furthermore, we choose the typical geological model for numerical modelling. We found out that the modelling results match the geological model reasonably well. Moreover, we use the method for detecting water bearing geological body in the roadway in the coalmine in Linfen city in Shanxi province, and the method can correctly locate the area of water bearing geological body. As a result, the present method can be feasibly and effectively applied in the disaster water source detection in coalmine roadway.

## ACKNOWLEDGMENT

The authors would like to thank three anonymous reviewers for critical reviews and comments.

## REFERENCES

[1] L. N. Pang, Q. X. Zhao, Kaiyue Zhao, "Predication of coalmine disaster water", *View Weekly*, vol. 22, pp. 17–17, 2011.

[2] Z. X. Liu, J. H. Yue, Y. G. Liu, "Application of sector detection technology in advanced detection", *Journal of China University of Mining and Technology*, vol. 36, no. 6, pp. 822–825, 2007. (in Chinese)

[3] J. L. Cheng, D. Chen, G. Q. Xue, "Synthetic aperture imaging in advanced detection of roadway using the mine transient electromagnetic method", *Chinese Journal of Geophysics,* vol. 59, no. 2, pp. 731–738, 2016. (in Chinese) Online. [Available]: https://www.doi.org/10.1002/cjg2.20225

[4] J. E. Danielsen, E. Auken, F. Jorgensen, "The application of the transient electromagnetic method in hydrogeophysical surveys", *Journal of Applied Geophysics*, vol. 53, pp. 181–198, 2003. Online. [Available]: https://doi.org/10.1016/j.jappgeo.2003.08.004

[5] A. Pethick, B. Harris, "Electromagnetic streamlines and the marine controlled source electromagnetic method", *Exploration Geophysics*, vol. 45, no. 3, pp. 208–215, 2014. Online. [Available]: https://doi.org/10.1071/EG13050

[6] I. J. Won, K. Smits, "Airborne electromagnetic bathymetry", *Geo. exploration*, vol. 27, no. 3, pp. 297–319, 1985. Online. [Available]: https://doi.org/10.1190/1.1442377

[7] J. C. Yu, *Mine Transient Electromagnetic Prospecting*. Xuzhou: Press of China University of Mining and Technology, 2007, ch. 2.

[8] A. A. Kaufman, G. V. Keller, *Frequency and Transient Sounding*. Elsevier Methods in Geochemistry & Geophysics, 1983, pp. 21.

[9] T. Wang, G. W. Hohmann, "A finite-difference time-domain solution for three-dimensional electromagnetic modeling", *Geophysics*, vol. 58, no. 6, pp. 797–809, 1993. Online. [Available]: https://doi.org/10.1190/1.1443465

[10] H. F. Sun, X. Li, S. C. Li, *et al*., "Three-dimensional FDTD modeling of TEM excited by a loop source considering ramp time", *Chinese Journal of Geophysics*, vol. 56, no. 3, pp. 1049–1064, 2013. (in Chinese). Online. [Available]: https://doi.org/10.6038/cjg20130333

[11] B. Y. Su, J. C. Yu, "Borehole electromagnetic method for exploration of coal mining goaf", *Elektronika ir Elektrotechnika*, vol. 22, no. 4, pp. 37–41, 2016. Online. [Available]: http://dx.doi.org/10.5755/j01.eie.22.4.15913